A Quantum Monte Carlo study of Electron-Positron Correlation in Silicon

Jan Härkönen

School of Science

Special assignment
Espoo 6.6.2019

Thesis supervisor:

Prof. Filip Tuomisto

Thesis advisor:

M.Sc. Kristoffer Simula

Aalto University
School of Science

Contents

Symbols and abbreviations

Symbols

$\mathbb{R}^n$	n-dimensional Euclidean space
$\mathbb{Z}^n$	set of integer valued n-dimensional vectors
$\mathbb{C}$	complex numbers

Operators

$\cdot$	dot product
$\lvert\cdot\rvert$	euclidean L^2 norm of a point
$\langle\cdot\rangle$	expectation value
Ψ^*	complex conjugate of Ψ
∇_i	nabla operator for ith particle

Abbreviations

QMC	Quantum Monte Carlo
VMC	Variational Monte Carlo
DFT	Density Functional Theory
PAS	Positron Annihilation Spectroscopy

1 Introduction

In this project we are working with positrons to characterize the defect structure of semiconductors. We use a method called "positron annihilation spectroscopy" (PAS) [10]. PAS is a method where we emit a positron to the semiconductor to detect positron annihilation radiation. In an imperfect atomic structure with missing atoms (vacancies) there will be a potential well where the vacancy is, where the positron can be further away from the repulsive nuclei and thus localizes into the vacancy. At the vacancy there will be a reduced local electron density, since on average the electrons are closer to the the atomic nuclei. The overlap of positrons and electrons within an imperfect atomic structure is lower than in a perfect one. These together increase the local positron density and prolongs the average lifetime of the positron and decreases the annihilation rate. In turn, we can determine how point defects affect some crucial properties of the semiconductor like mechanical properties, electrical conductivity, diffusivity, or light emission.

There is a widely used technique for computational quantum mechanic modelling called density functional theory (DFT) [1,8,10]. However DFT needs functionals and approximations with too many parameters. DFT doesn't describe momentum-space quantities such as the momentum density of annihilating electron-positron pairs or properly take into account electron-electron or electron-positron correlation or the local behaviour of particles of the exact wave function. Monte Carlo methods are a good way of calculating physical expectation values by approximating directly the interacting many-body wave function.

In this assignment we concentrate on the simulations of PAS, by using Quantum Monte Carlo (QMC) methods. The Variational Monte Carlo (VMC) is a QMC method for calculating high-dimensional integrals by calculating the expectation value for some property of an atomic structure by using random samples for a chosen trial wave function. For example, in order to calculate the annihilation rate of positrons (more on this in 3.2), we need to simulate the correlated density of electrons at the positron's site. In this special assignment we are going to simulate and visualize both the contact pair correlation function and the so-called enhancement factor in a simulation atomic lattice between two atoms. Then we will compare the results to the predictions of the local-density approximation. To do this we are first going to introduce the theory behind the calculations in 3 and present the silicon lattice used to execute the calculations in 4.1, after which we present how to visualize our results 4.3.

2 Basic concepts

2.1 Defining variables

Let $\{\boldsymbol{r}_1, \ldots, \boldsymbol{r}_N\}$ be the electron's positions, where $\boldsymbol{r}_i \in \mathbb{R}^3$, $i \in \{1, \ldots, N\}$. Let $\boldsymbol{r}_0 \in \mathbb{R}^3$ be the positron's position. Let $\Psi(\boldsymbol{r}_1, \ldots, \boldsymbol{r}_N)$ be the wave function of a system of N electrons and $\Psi(\boldsymbol{r}_0; \boldsymbol{r}_1, \ldots, \boldsymbol{r}_N)$ be the wave function of a system of N

electrons and one positron. Let

$$R' = (\boldsymbol{r}_2, \ldots, \boldsymbol{r}_N) \in \mathbb{R}^{3\times(N-1)} \tag{1}$$
$$R = (\boldsymbol{r}_1, \ldots, \boldsymbol{r}_N) \in \mathbb{R}^{3\times N} \tag{2}$$
$$R^+ = (\boldsymbol{r}_0, \ldots, \boldsymbol{r}_N) \in \mathbb{R}^{3\times(N+1)} \tag{3}$$

such that

$$\Psi(R) = \Psi(\boldsymbol{r}_1, \ldots, \boldsymbol{r}_N) \tag{4}$$

and

$$\Psi(\boldsymbol{r}_0; \boldsymbol{r}_1, \ldots, \boldsymbol{r}_N) = \Psi(\boldsymbol{r}_0; \boldsymbol{r}_1, R') = \Psi(\boldsymbol{r}_0; R) = \Psi(R^+) = \Psi. \tag{5}$$

Also let

$$\mathrm{d}\boldsymbol{r}_0\,\mathrm{d}\boldsymbol{r}_1 \ldots \mathrm{d}\boldsymbol{r}_N = \mathrm{d}\boldsymbol{r}_0\,\mathrm{d}\boldsymbol{r}_1\,\mathrm{d}R' = \mathrm{d}\boldsymbol{r}_0\,\mathrm{d}R = \mathrm{d}R^+. \tag{6}$$

Let the distance between particle i and j be

$$r_{ij} = |\boldsymbol{r}_i - \boldsymbol{r}_j|. \tag{7}$$

Let the position of the ith particle be

$$\boldsymbol{r}_i = \begin{bmatrix} r_{ix} \\ r_{iy} \\ r_{iz} \end{bmatrix}. \tag{8}$$

Then the nabla operator for the ith particle $\nabla_i : \mathbb{R} \to \mathbb{R}^3$ is defined as

$$\nabla_i = \begin{bmatrix} \partial/\partial r_{ix} \\ \partial/\partial r_{iy} \\ \partial/\partial r_{iz} \end{bmatrix}. \tag{9}$$

Also the Laplace operator for the ith particle $\nabla_i^2 : \mathbb{R} \to \mathbb{R}$ is defined as

$$\nabla_i^2 = \frac{\partial^2}{\partial r_{ix}^2} + \frac{\partial^2}{\partial r_{iy}^2} + \frac{\partial^2}{\partial r_{iz}^2} \tag{10}$$

2.2 Variational Monte Carlo

The main benefit of using the Monte Carlo method is to solve high-dimensional integrals which would otherwise require unreasonable computing power. The principle behind QMC is that we can efficiently calculate the expectation value of any operator $\hat{O}$. Our simulation's main calculation method is called variational Monte Carlo (VMC). It is a method that iterates the trial wave function to be more and more accurate by using quantum mechanical variational principle and energy minimization.

More details about this can be found on the paper [7] or [5]. The expectation value for operator $\hat{O}$ is

$$\langle \hat{O} \rangle_{VMC} = \frac{\langle \Psi | \hat{O} | \Psi \rangle}{\langle \Psi | \Psi \rangle} = \frac{\int \Psi^*(R) \hat{O} \Psi(R) \, \mathrm{d}R}{\int \Psi^*(R) \Psi(R) \, \mathrm{d}R} = \frac{\int |\Psi(R)|^2 \hat{O}_{loc}(R) \, \mathrm{d}R}{\int |\Psi(R)|^2 \, \mathrm{d}R}, \tag{11}$$

where $\hat{O}_{loc}(R)$ is the local value of the operator $\hat{O}$ in R, such that

$$\hat{O}_{loc}(R) = \frac{\hat{O}\Psi(R)}{\Psi(R)}. \tag{12}$$

When $|\Psi|^2$ is normalized, then the expectation value can be expressed in a simpler form

$$\langle \hat{O} \rangle_{VMC} = \langle \Psi | \hat{O} | \Psi \rangle = \int |\Psi(R)|^2 \hat{O}_{loc}(R) \, \mathrm{d}R \tag{13}$$

Because $|\Psi(R)|^2$ is considered to be the probability density function over R, we can approximate $\langle \hat{O} \rangle$ with the Monte Carlo method by randomly sampling M times a configuration R_i from the $|\Psi|^2$ distribution and calculating the average of every local value of the operator:

$$\langle \hat{O} \rangle_{VMC} \approx \frac{1}{M} \sum_{i=1}^{M} \hat{O}_{loc}(R_i). \tag{14}$$

And the sample error for the mean of the operator $\hat{O}$ is

$$\Delta \langle \hat{O} \rangle_{VMC} = \sqrt{\frac{\langle \hat{O}^2 \rangle_{VMC} - \langle \hat{O} \rangle_{VMC}^2}{M - 1}} \tag{15}$$

The more configurations we have, the more accurate our results are. In the limit $M \to \infty$ we get the exact value of the expectation value $\langle \hat{O} \rangle_{VMC}$ and the error $\Delta \langle \hat{O} \rangle_{VMC}$ tends to zero.

2.3 CASINO

CASINO is the simulation program used for the calculations. It was originally developed in Cambridge university and can be downloaded from their website. It was developed specifically to calculate a broad variety of quantum mechanical properties of different structures on the atomic scale using QMC methods.

2.4 Slater-Jastrow wave function

The wave function of a system with 1 or 2 electrons can be solved analytically using the Schrödinger's equation quite easily. However, when we go beyond 2 electrons, solving the wave function analytically gets increasingly more complicated. Some of our systems involve up to 64 electrons. Calculating an analytical wave function for such systems is practically impossible. To circumvent this problem, we use an

approximation for the wave function called the Slater-Jastrow wave function found in [5] equation (4.1) or in [7]:

$$\Psi(R^+) \approx e^{J(R^+)} D_\uparrow(R_\uparrow) D_\downarrow(R_\downarrow) \phi_0(\boldsymbol{r}_0). \tag{16}$$

The terms $D_\uparrow(R_\uparrow)$ and $D_\downarrow(R_\downarrow)$ are the Slater determinants of occupied single particle orbitals ϕ_i for particles with up and down spins respectively. The term $\phi_0(\boldsymbol{r}_0)$ is the orbital for the positron. Let the number of particles with up spin be $N_\uparrow$ and for down spin $N_\downarrow$, so the total number of particles is $N = N_\uparrow + N_\downarrow$. The Slater determinants are defined as follows:

$$D_\uparrow(R_\uparrow) = D_\uparrow(\boldsymbol{r}_1, \ldots, \boldsymbol{r}_{N_\uparrow}) = \begin{vmatrix} \phi_1(\boldsymbol{r}_1) & \ldots & \phi_1(\boldsymbol{r}_{N_\uparrow}) \\ \vdots & \ddots & \vdots \\ \phi_{N_\uparrow}(\boldsymbol{r}_1) & \ldots & \phi_{N_\uparrow}(\boldsymbol{r}_{N_\uparrow}) \end{vmatrix}. \tag{17}$$

and

$$D_\downarrow(R_\downarrow) = D_\downarrow(\boldsymbol{r}_{N_\uparrow+1}, \ldots, \boldsymbol{r}_N) = \begin{vmatrix} \phi_{N_\uparrow+1}(\boldsymbol{r}_{N_\uparrow+1}) & \ldots & \phi_{N_\uparrow+1}(\boldsymbol{r}_N) \\ \vdots & \ddots & \vdots \\ \phi_N(\boldsymbol{r}_{N_\uparrow+1}) & \ldots & \phi_{N_\uparrow}(\boldsymbol{r}_N) \end{vmatrix}. \tag{18}$$

The term $J(R^+)$ is the Jastrow factor. If we only include the single- and two-particle terms, the Jastrow factor is

$$J(R^+) = J(\boldsymbol{r}_0, \ldots, \boldsymbol{r}_N) = \sum_i \chi(\boldsymbol{r}_i) - \sum_{i<j} u(|\boldsymbol{r}_i - \boldsymbol{r}_j|). \tag{19}$$

The Jastrow factor can have more terms in order to get a more accurate wave function, but often it is enough to use only these two terms. The term χ characterizes the correlations between the nucleus and an electron (or positron). The term u characterizes the electron-electron (or electron-positron) correlations. Both terms χ and u are functions that decay as a function of distance. More details of what the terms χ and u represent can be found e.g. on Foulkes-Mitas-Needs-Rajagopal's paper [5] or on Drummond-Towler-Needs' paper [4]. Recall that the nonrelativistic Born-Oppenheimer Hamiltonian operator was defined as

$$\hat{H} = -\frac{1}{2}\sum_i \nabla_i^2 - \sum_i \sum_\alpha \frac{Z_\alpha}{|\boldsymbol{r}_i - \boldsymbol{d}_\alpha|} + \frac{1}{2}\sum_i \sum_{i \neq j} \frac{1}{|\boldsymbol{r}_i - \boldsymbol{r}_j|}. \tag{20}$$

This operator can be used in VMC to calculate the energy, which we want to minimize by tweaking the parameters of the Jastrow factor. We do this to obtain an optimized Slater-Jastrow wave function for accurate simulations. We also need relativistic corrections in order to calculate the pseudopotentials, even though they are small. Details in [5].

2.5 Positron annihilation spectroscopy

Positron annihilation spectroscopy (PAS [10]) is a method that allows us to identify defects in semiconductors on an atomic scale. To achieve this we inject positrons

originating from a Na^{22} sample onto the semiconductor we want to analyze. Once the positron has reached the semiconductor, it thermalizes, and eventually collides with an electron and both the electron and positron annihilates and emits two γ-quanta of 511 keV, which can be detected. To acquire the annihilation lifetime spectrum, we first use a start signal which comes from the Na^{22} source. Then we use the annihilation signal, which is detected practically simultaneously along with the start signal. Then the distribution of the time difference between the signals reflects the lifetime of a positron in the sample. The rate of annihilation λ can also be calculated by taking its inverse value of the average lifetime $\lambda = \frac{1}{\tau}$ of a positron which usually lies within range of 100-500 ps.

For the atomic structure we can predict an average lifetime of the positron for different sorts of defects or amounts of vacancies. Thus for a sample we can make measurements for the average lifetime of a positron so that we can get an idea of what kind of structure the sample has.

3 Contact pair correlation function

3.1 Contact density

Let's first start with a simpler concept we call here contact density. Assuming Ψ^2 is normalized, let's first compute the system-wide expectation value of the Dirac delta function

$$\left\langle \delta(r_{i0}) \right\rangle = \int \Psi^* \delta(r_{i0}) \Psi \, \mathrm{d}R^+ = \int \Psi^2 \delta(r_{i0}) \, \mathrm{d}R^+. \tag{21}$$

Using Bressanini-Mella-Morosi's paper's [2] identity (11) for the Dirac delta function, its expectation value can be computed

$$\int \Psi^2 \delta(r_{i0}) \, \mathrm{d}R^+ = -\frac{1}{4\pi} \int \Psi^2 \nabla_i^2 \frac{1}{r_{i0}} \, \mathrm{d}R^+. \tag{22}$$

Now by integrating by parts twice we get

$$-\frac{1}{4\pi} \int \Psi^2 \nabla_i^2 \frac{1}{r_{i0}} \, \mathrm{d}R^+ \tag{23}$$

$$= -\frac{1}{4\pi} \int \nabla_i^2 \Psi^2 \frac{1}{r_{i0}} \, \mathrm{d}R^+ \tag{24}$$

$$= -\frac{1}{2\pi} \int \Psi^2 \left[\frac{\nabla_i^2 \Psi}{\Psi} + \left| \frac{\nabla_i \Psi}{\Psi} \right|^2 \right] \frac{1}{r_{j0}} \, \mathrm{d}R^+ \tag{25}$$

$$= -\frac{1}{2\pi} \int \Psi^2 \left[\frac{\nabla_i^2 \Psi}{\Psi} + |\nabla_i \ln \Psi|^2 \right] \frac{1}{r_{j0}} \, \mathrm{d}R^+. \tag{26}$$

This result is the same as the result in [2] equation 14 . Next we compute the formula for contact density, which can be evaluated with QMC. Contact density is

$$CD = \left\langle \sum_{i=1}^{N} \delta(r_{i0}) \right\rangle \tag{27}$$

Let's use the identity 10 in Kenny-Rajagopal-Needs' paper [6] but by slightly changing the summation indexing. Let the set of indexes for i and j be

$$I^+ = \{0, \ldots, N\} \times \{1, \ldots, N\} \quad \text{and} \tag{28}$$

$$I = \{1, \ldots, N\} \times \{1, \ldots, N\} \tag{29}$$

We get

$$CD = \Big\langle \sum_{i=1}^{N} \delta(r_{i0}) \Big\rangle = \Big\langle -\frac{1}{4\pi} \Big[\sum_{i=0}^{N} \nabla_i^2 \Big] \Big[\frac{1}{2} \sum_{j=1}^{N} \frac{1}{r_{j0}} \Big] \Big\rangle \tag{30}$$

$$= -\frac{1}{8\pi} \sum_{(i,j)\in I^+} \Big\langle \nabla_i^2 \frac{1}{r_{j0}} \Big\rangle \tag{31}$$

$$= -\frac{1}{4\pi} \sum_{(i,j)\in I^+} \int \Psi^2 \Big[\frac{\nabla_i^2 \Psi}{\Psi} + |\nabla_i \ln \Psi|^2 \Big] \frac{1}{r_{j0}} \, \mathrm{d}R^+ \tag{32}$$

Let the drift velocity of the i:th particle be $V_i \in \mathbb{R}^3$. Let the kinetic energy of the i:th particle be K_i, which are defined as follows:

$$V_i = \frac{\nabla_i \Psi}{\Psi} = \nabla_i \ln \Psi \tag{33}$$

$$K_i = -\frac{1}{2} \frac{\nabla_i^2 \Psi}{\Psi}. \tag{34}$$

Moving on from expression (32), we get

$$CD = -\frac{1}{4\pi} \sum_{(i,j)\in I^+} \int \Psi^2 \Big[\frac{\nabla_i^2 \Psi}{\Psi} + |\nabla_i \ln \Psi|^2 \Big] \frac{1}{r_{j0}} \, \mathrm{d}R^+ \tag{35}$$

$$= \frac{1}{2\pi} \sum_{(i,j)\in I^+} \int \Psi^2 \Big[-\frac{1}{2} \frac{\nabla_i^2 \Psi}{\Psi} - \frac{1}{2} |\nabla_i \ln \Psi|^2 \Big] \frac{1}{r_{j0}} \, \mathrm{d}R^+ \tag{36}$$

$$= \frac{1}{2\pi} \sum_{(i,j)\in I^+} \int \Psi^2 \Big[K_i - \frac{1}{2} |V_i|^2 \Big] \frac{1}{r_{j0}} \, \mathrm{d}R^+ \tag{37}$$

$$= \frac{1}{2\pi} \int \Psi^2 \Big[\sum_{i=0}^{N} K_i - \frac{1}{2} |V_i|^2 \Big] \Big[\sum_{j=1}^{N} \frac{1}{r_{j0}} \Big] \, \mathrm{d}R^+ \tag{38}$$

$$= \Big\langle \frac{1}{2\pi} \Big[\sum_{i=0}^{N} K_i - \frac{1}{2} |V_i|^2 \Big] \Big[\sum_{j=1}^{N} \frac{1}{r_{j0}} \Big] \Big\rangle \tag{39}$$

This result can be acquired using the random configurations in QMC according to the probability density function Ψ^2.

3.2 Contact pair correlation function

In order to calculate the positron annihilation rate λ and the positron's average lifetime τ with DFT, we have the following formula:

$$\lambda = \frac{1}{\tau} = \pi r_e^2 c \int n_+(\boldsymbol{r}_0) n_-(\boldsymbol{r}_0) g(\boldsymbol{r}_0, \boldsymbol{r}_0; [n_+, n_-]) \, \mathrm{d}\boldsymbol{r}_0. \tag{40}$$

The formula is from Borosńki-Nieminen's paper [1]. Let's break down all the elements in the formula. The variable r_e is the classical radius of the electron and c is the speed of light. The single-particle densities of the electrons and positrons at a point in 3D space $\boldsymbol{r}_0 \in \mathbb{R}^3$ is expressed with $n_-(\boldsymbol{r}_0)$ and $n_+(\boldsymbol{r}_0)$ respectively. However, these factors do not include the correlations of the many-body wave function. Therefore we need an enhancement factor $g(\boldsymbol{r}_0, \boldsymbol{r}_0; [n_+, n_-])$ for more accurate calculations. The enhancement factor expresses the electron-positron pair correlation function $g(\boldsymbol{r}_0, \boldsymbol{r}_0'; [n_+, n_-])$ at zero distance. From this point onward all calculations will be done in order to simulate the whole contact pair correlation function of the integral in (40). For the sake of clearer notation, let's express this contact pair correlation function as a function $f : \mathbb{R}^3 \to \mathbb{R}$ such that

$$f(\boldsymbol{r}_0) := n_+(\boldsymbol{r}_0) n_-(\boldsymbol{r}_0) g(\boldsymbol{r}_0, \boldsymbol{r}_0; [n_+, n_-]). \tag{41}$$

If we wanted to express this in a VMC-friendly format it would looks like this:

$$f(\boldsymbol{r}_0) = \left\langle \sum_{i=1}^{N} \delta(\boldsymbol{r}_{i0}) \right\rangle \tag{42}$$

3.3 The contact pair correlation function in momentum space

The contact pair correlation function $f(\boldsymbol{r}_0)$ in momentum space can be acquired by performing a Fourier-transform to f. Let this Fourier transform be a function $\hat{f} : \mathbb{R}^3 \to \mathbb{C}$ defined as

$$\hat{f}(\boldsymbol{p}) = \frac{1}{|V|} \int_V e^{-i\boldsymbol{p}\cdot\boldsymbol{r}_0} f(\boldsymbol{r}_0) \, \mathrm{d}\boldsymbol{r}_0. \tag{43}$$

The set V is the area inside the simulation lattice, whose volume is $|V|$. The term $\hat{f}$ can be calculated in a QMC-friendly format:

$$\hat{f}(\boldsymbol{p}) = \left\langle \sum_{i=1}^{N} e^{-i\boldsymbol{p}\cdot\boldsymbol{r}_0} \delta(\boldsymbol{r}_{i0}) \right\rangle. \tag{44}$$

For readability's sake we shall use the abbreviation $e_0 = e^{-i\boldsymbol{p}\cdot\boldsymbol{r}_0}$. Therefore the following statements hold:

$$\nabla_0 e_0 = \nabla_0 (e^{-i\boldsymbol{p}\cdot\boldsymbol{r}_0}) = -i\boldsymbol{p} e^{-i\boldsymbol{p}\cdot\boldsymbol{r}_0} = -i\boldsymbol{p} e_0, \tag{45}$$

$$\nabla_0^2 e_0 = \nabla_0^2 (e^{-i\boldsymbol{p}\cdot\boldsymbol{r}_0}) = -|\boldsymbol{p}|^2 e^{-i\boldsymbol{p}\cdot\boldsymbol{r}_0} = -|\boldsymbol{p}|^2 e_0. \tag{46}$$

Recall in (9) and (10) how the nabla operator and Laplace operator were defined. Now let's first compute

$$\hat{f}(\boldsymbol{p}) = \Big\langle \sum_{i=1}^{N} e_0 \delta(r_{i0}) \Big\rangle \tag{47}$$

$$= \int \Psi^2 \sum_{i=0}^{N} e_0 \delta(r_{i0}) \, \mathrm{d}R^+ \tag{48}$$

$$= -\frac{1}{4\pi} \int \Psi^2 \Big[\sum_{i=0}^{N} e_0 \nabla_i^2 \Big] \Big[\frac{1}{2} \sum_{j=1}^{N} \frac{1}{r_{j0}} \Big] \, \mathrm{d}R^+ \tag{49}$$

$$= -\frac{1}{8\pi} \sum_{(i,j)\in I^+} \int \Psi^2 e_0 \nabla_i^2 \frac{1}{r_{j0}} \, \mathrm{d}R^+, \tag{50}$$

Where I^+ is defined in (28). Let's integrate by parts twice.

$$-\frac{1}{8\pi} \sum_{(i,j)\in I^+} \int \Psi^2 e_0 \nabla_i^2 \frac{1}{r_{j0}} \, \mathrm{d}R^+ \tag{51}$$

$$= -\frac{1}{8\pi} \sum_{(i,j)\in I^+} \int \nabla_i^2 (\Psi^2 e_0) \frac{1}{r_{j0}} \, \mathrm{d}R^+ \tag{52}$$

$$= -\frac{1}{8\pi} \sum_{(i,j)\in I^+} \int \Big[e_0 \nabla_i^2 \Psi^2 + 2 \nabla_i e_0 \cdot \nabla_i \Psi^2 + \Psi^2 \nabla_i^2 e_0 \Big] \frac{1}{r_{j0}} \, \mathrm{d}R^+ \tag{53}$$

Let's use the definitions (29) for I to break down I^+.

$$\hat{f}(\boldsymbol{p}) = \Big\langle \sum_{i=1}^{N} e_0 \delta(r_{i0}) \Big\rangle \tag{54}$$

$$- \frac{1}{8\pi} \sum_{(i,j)\in I^+} \int \Big[e_0 \nabla_i^2 \Psi^2 + 2\nabla_i e_0 \cdot \nabla_i \Psi^2 + \Psi^2 \nabla_i^2 e_0 \Big] \frac{1}{r_{j0}} \, \mathrm{d}R^+ \tag{55}$$

$$= - \frac{1}{8\pi} \Big[\sum_{(i,j)\in I} \int \Big[e_0 \nabla_i^2 \Psi^2 + 2 \underbrace{\nabla_i e_0}_{=0} \cdot \nabla_i \Psi^2 + \Psi^2 \underbrace{\nabla_i^2 e_0}_{=0} \Big] \frac{1}{r_{j0}} \, \mathrm{d}R^+ \tag{56}$$

$$+ \sum_{j=1}^{N} \int \Big[e_0 \nabla_0^2 \Psi^2 + 2\nabla_0 e_0 \cdot \nabla_0 \Psi^2 + \Psi^2 \nabla_0^2 e_0 \Big] \frac{1}{r_{j0}} \, \mathrm{d}R^+ \Big] \tag{57}$$

$$= - \frac{1}{8\pi} \int \Big[\sum_{i=1}^{N} \Big[e_0 \nabla_i^2 \Psi^2 \Big] + e_0 \nabla_0^2 \Psi^2 + 2\nabla_0 e_0 \cdot \nabla_0 \Psi^2 + \Psi^2 \nabla_0^2 e_0 \Big] \Big[\sum_{j=1}^{N} \frac{1}{r_{j0}} \Big] \, \mathrm{d}R^+ \tag{58}$$

$$= - \frac{1}{8\pi} \int \Big[\sum_{i=0}^{N} \Big[e_0 \nabla_i^2 \Psi^2 \Big] - 2 e_0 i\boldsymbol{p} \cdot 2\Psi \nabla_0 \Psi - |\boldsymbol{p}|^2 \Psi^2 e_0 \Big] \Big[\sum_{j=1}^{N} \frac{1}{r_{j0}} \Big] \, \mathrm{d}R^+ \tag{59}$$

$$= - \frac{1}{8\pi} \int e_0 \Big[\sum_{i=0}^{N} \Big[\nabla_i^2 \Psi^2 \Big] - 4\Psi i\boldsymbol{p} \cdot \nabla_0 \Psi - |\boldsymbol{p}|^2 \Psi^2 \Big] \Big[\sum_{j=1}^{N} \frac{1}{r_{j0}} \Big] \, \mathrm{d}R^+ \tag{60}$$

$$= - \frac{1}{8\pi} \int e_0 \Big[2 \sum_{i=0}^{N} \Big[\Psi \nabla_i^2 \Psi + |\nabla_i \Psi|^2 \Big] - 4\Psi i\boldsymbol{p} \cdot \nabla_0 \Psi - |\boldsymbol{p}|^2 \Psi^2 \Big] \Big[\sum_{j=1}^{N} \frac{1}{r_{j0}} \Big] \, \mathrm{d}R^+ \tag{61}$$

$$= \frac{1}{2\pi} \int \Psi^2 e_0 \Big[\sum_{i=0}^{N} \Big[- \frac{1}{2} \frac{\nabla_i^2 \Psi}{\Psi} - \frac{1}{2} |\nabla_i \ln \Psi|^2 \Big] + i\boldsymbol{p} \cdot \nabla_0 \ln \Psi + \frac{1}{4} |\boldsymbol{p}|^2 \Big] \Big[\sum_{j=1}^{N} \frac{1}{r_{j0}} \Big] \, \mathrm{d}R^+ \tag{62}$$

$$= \frac{1}{2\pi} \int \Psi^2 e_0 \Big[\sum_{i=0}^{N} \Big[K_i - \frac{1}{2} |V_i|^2 \Big] + i\boldsymbol{p} \cdot V_0 + \frac{1}{4} |\boldsymbol{p}|^2 \Big] \Big[\sum_{j=1}^{N} \frac{1}{r_{j0}} \Big] \, \mathrm{d}R^+ \tag{63}$$

$$= \frac{1}{2\pi} \int \Psi^2 \underbrace{e^{-i\boldsymbol{p}\cdot\boldsymbol{r}_0} \Big[\sum_{i=0}^{N} \Big[K_i - \frac{1}{2} |V_i|^2 \Big] + i\boldsymbol{p} \cdot V_0 + \frac{1}{4} |\boldsymbol{p}|^2 \Big]}_{=A+Bi} \underbrace{\Big[\sum_{j=1}^{N} \frac{1}{r_{j0}} \Big]}_{=S} \, \mathrm{d}R^+ \tag{64}$$

This is now the contact pair correlation function in the momentum space, which can be sampled easily using the drift velocity V_i and the kinetic energy K_i. Let's examine $A + Bi$ and break it down to its real and complex component:

$$A + Bi = e^{-i\boldsymbol{p}\cdot\boldsymbol{r}_0} \Big[\sum_{i=0}^{N} \Big[K_i - \frac{1}{2} |V_i|^2 \Big] + i\boldsymbol{p} \cdot V_0 + \frac{1}{4} |\boldsymbol{p}|^2 \Big] \tag{65}$$

$$= \Big[cos(\boldsymbol{p} \cdot \boldsymbol{r}_0) - isin(\boldsymbol{p} \cdot \boldsymbol{r}_0) \Big] \Big[\sum_{i=0}^{N} \Big[K_i - \frac{1}{2} |V_i|^2 \Big] + i\boldsymbol{p} \cdot V_0 + \frac{1}{4} |\boldsymbol{p}|^2 \Big] \tag{66}$$

so

$$A = cos(\boldsymbol{p}\cdot\boldsymbol{r}_0)\Big[\sum_{i=0}^{N}\Big[K_i - \frac{1}{2}|V_i|^2\Big] + \frac{1}{4}|\boldsymbol{p}|^2\Big] + sin(\boldsymbol{p}\cdot\boldsymbol{r}_0)\boldsymbol{p}\cdot V_0 \tag{67}$$

$$B = -sin(\boldsymbol{p}\cdot\boldsymbol{r}_0)\Big[\sum_{i=0}^{N}\Big[K_i - \frac{1}{2}|V_i|^2\Big] + \frac{1}{4}|\boldsymbol{p}|^2\Big] + cos(\boldsymbol{p}\cdot\boldsymbol{r}_0)\boldsymbol{p}\cdot V_0 \tag{68}$$

Because the integral (64) involves the probability distribution Ψ^2, the term $\hat{f}$ can be considered as being the expectation value

$$\hat{f}(\boldsymbol{p}) = \frac{\langle AS\rangle + i\langle BS\rangle}{2\pi}. \tag{69}$$

The more configurations we have, the more accurate are the results.

4 Simulations

4.1 Simulation lattices used

Next we're going to simulate the contact pair correlation function in the momentum space and visualize it on a 1-dimensional line with CASINO using QMC. The simulation lattice we're using is a silicon (Si) periodic lattice in a face-centered cubic (FCC) structure, where the primitive lattice vectors are

$$\begin{bmatrix}\boldsymbol{r}_1 & \boldsymbol{r}_2 & \boldsymbol{r}_3\end{bmatrix} = 5.130606\begin{bmatrix}1 & 0 & 1\\ 1 & 1 & 0\\ 0 & 1 & 1\end{bmatrix}. \tag{70}$$

The lattice contains 2 atoms, whose positions are

$$\mathbf{0} = \begin{bmatrix}0\\0\\0\end{bmatrix} \quad \text{and} \quad \frac{1}{4}(\boldsymbol{r}_1+\boldsymbol{r}_2+\boldsymbol{r}_3) = 5.130606\begin{bmatrix}1/2\\1/2\\1/2\end{bmatrix} \tag{71}$$

The corresponding reciprocal lattice vectors are

$$\begin{bmatrix}\boldsymbol{p}_1 & \boldsymbol{p}_2 & \boldsymbol{p}_3\end{bmatrix} = 0.612323895772\begin{bmatrix}1 & -1 & 1\\ 1 & 1 & -1\\ -1 & 1 & 1\end{bmatrix}, \tag{72}$$

where the numbers are expressed in atomic units (a.u.). This implies that

$$\boldsymbol{r}_i\cdot\boldsymbol{p}_j = \begin{cases}2\pi, & \text{if } i=j\\ 0, & \text{if } i\neq j\end{cases} \tag{73}$$

When examining the contact pair correlation function in momentum space, we define the momentum component

$$\boldsymbol{p}_{nml} = n\boldsymbol{p}_1 + m\boldsymbol{p}_2 + l\boldsymbol{p}_3, \tag{74}$$

where n, m and l are integers. Thus we can create a discrete 3D function $\lambda : \mathbb{Z}^3 \to \mathbb{C}$ such that

$$\lambda(n, m, l) = \hat{f}(\boldsymbol{p}_{nml}) = \hat{f}(n\boldsymbol{p}_1 + m\boldsymbol{p}_2 + l\boldsymbol{p}_3). \tag{75}$$

4.2 Monte Carlo simulation

After running the simulations we want to check if the acquired values actually converge. Let λ_R and λ_C be the real and complex components of λ as shown in (69) such that $\lambda_R, \lambda_C : \mathbb{Z}^3 \to \mathbb{R}$ and

$$\lambda(n, m, l) = \lambda_R(n, m, l) + i \cdot \lambda_C(n, m, l). \tag{76}$$

Let's examine the convergence different values of λ:

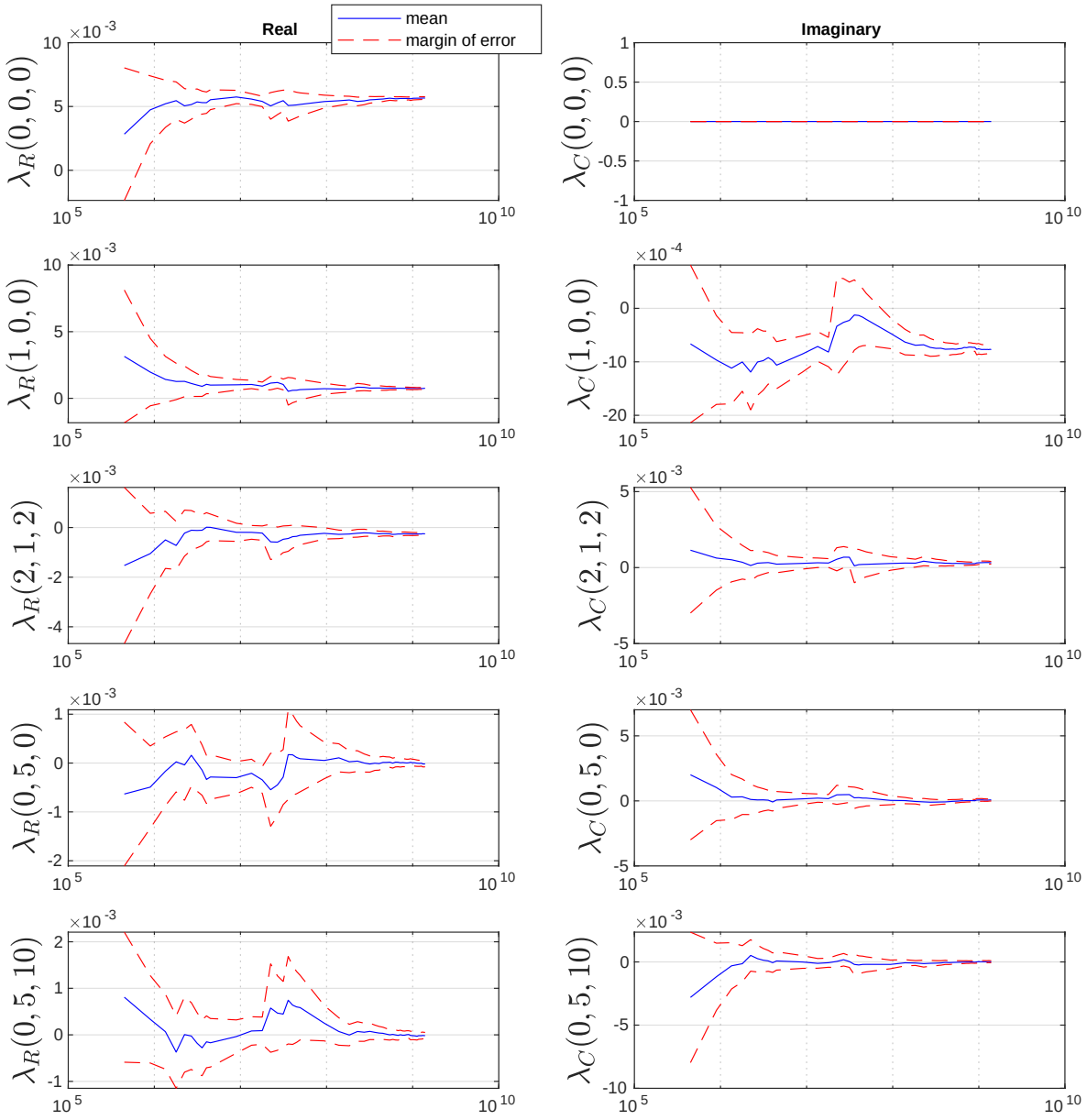

Figure 1: Convergence of contact pair correlation function when the number of configurations increase.

Based on these observations, we can confidently say that all values for λ do indeed converge. Let's see what that graph looks like in one dimension:

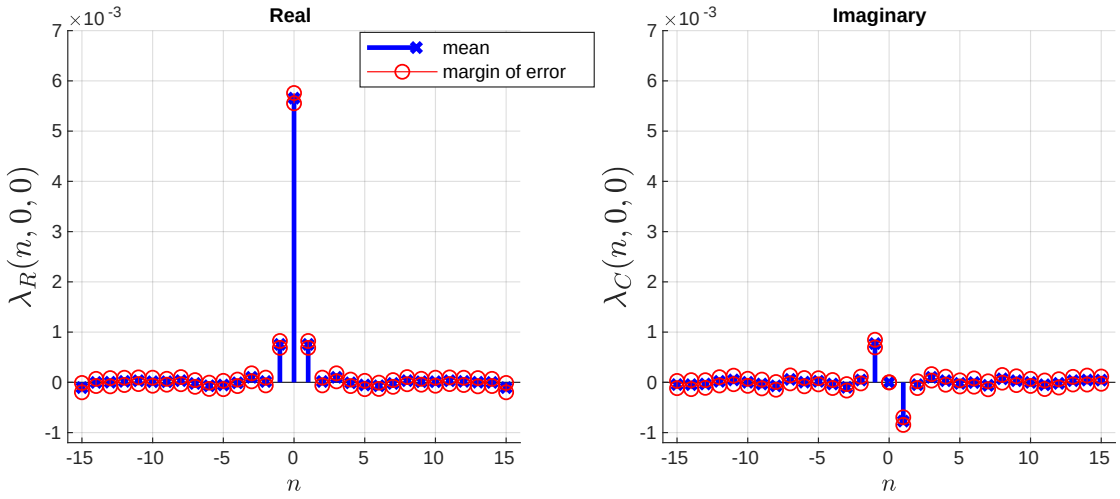

Figure 2: Both real and imaginary values for λ, when the 2 last parameters are fixed to 0 so that we get a 1D graph.

All of these figures use two times the sample error calculated in (15) as the margin of error, which is roughly equivalent to the 95% confidence interval.

4.3 How to obtain the contact pair correlation function in real space

Because the atomic structure is periodic, it has to be translation invariant. Let's choose any 3 integers a_1, a_2 and a_3. Then

$$f(\boldsymbol{r}_0 + a_1\boldsymbol{r}_1 + a_2\boldsymbol{r}_2 + a_3\boldsymbol{r}_3) = f(\boldsymbol{r}_0). \tag{77}$$

Also

$$cos(\boldsymbol{p}\cdot(\boldsymbol{r}_0 + a_1\boldsymbol{r}_1 + a_2\boldsymbol{r}_2 + a_3\boldsymbol{r}_3)) = cos(\boldsymbol{p}\cdot\boldsymbol{r}_0). \tag{78}$$

We can state the same thing for the *sin* function with the same logic. Define the total momentum $\boldsymbol{p}$ used in the Fourier transform in (43) as

$$\boldsymbol{p}_{nml} = n\boldsymbol{p}_1 + m\boldsymbol{p}_2 + l\boldsymbol{p}_3 \tag{79}$$

exactly as in (74). Then we can express any position $\boldsymbol{r}_0$ in the simulation lattice with

$$\boldsymbol{r}_0(t_1,t_2,t_3) = t_1\boldsymbol{r}_1 + t_2\boldsymbol{r}_2 + t_3\boldsymbol{r}_3 \tag{80}$$

such that $t_1, t_2, t_3 \in [0,1]$. Then

$$\begin{aligned}\boldsymbol{p}_{nml}\cdot\boldsymbol{r}_0(t_1,t_2,t_3) =& (n\boldsymbol{p}_1 + m\boldsymbol{p}_2 + l\boldsymbol{p}_3)\cdot(t_1\boldsymbol{r}_1 + t_2\boldsymbol{r}_2 + t_3\boldsymbol{r}_3) &(81)\\ =& nt_1\boldsymbol{p}_1\cdot\boldsymbol{r}_1 + mt_2\boldsymbol{p}_2\cdot\boldsymbol{r}_2 + lt_3\boldsymbol{p}_3\cdot\boldsymbol{r}_3 &(82)\\ =& 2\pi(nt_1 + mt_2 + lt_3). &(83)\end{aligned}$$

According to (77) the contact pair correlation function is periodic, therefore we can express the contact pair correlation function f as a linear combination of *sin* and *cos* functions:

$$f(\boldsymbol{r}_0) = \sum_{(n,m,l)\in\mathbb{Z}^3} a_{nml} cos(\boldsymbol{p}_{nml} \cdot \boldsymbol{r}_0) + b_{nml} sin(\boldsymbol{p}_{nml} \cdot \boldsymbol{r}_0). \tag{84}$$

Let's express the contact pair correlation function like this:

$$\begin{aligned}
&\gamma(t_1, t_2, t_3) && (85)\\
=&f(\boldsymbol{r}_0(t_1, t_2, t_3)) && (86)\\
=&\sum_{(n,m,l)\in\mathbb{Z}^3} a_{nml} cos(\boldsymbol{p}_{nml} \cdot \boldsymbol{r}_0(t_1, t_2, t_3)) + b_{nml} sin(\boldsymbol{p}_{nml} \cdot \boldsymbol{r}_0(t_1, t_2, t_3)) && (87)\\
=&\sum_{(n,m,l)\in\mathbb{Z}^3} a_{nml} cos(2\pi(nt_1 + mt_2 + lt_3)) + b_{nml} sin(2\pi(nt_1 + mt_2 + lt_3)). && (88)
\end{aligned}$$

Now let's express the contact pair correlation function in the momentum space. We can use (75) and (43) to express

$$\lambda(n, m, l) = \hat{f}(\boldsymbol{p}_{nml}) = \frac{1}{|V|} \int_V e^{-i\boldsymbol{p}_{nml}\cdot\boldsymbol{r}_0} f(\boldsymbol{r}_0)\, \mathrm{d}\boldsymbol{r}_0. \tag{89}$$

By doing a variable change from $\boldsymbol{r}_0$ to $\boldsymbol{r}_0(t_1, t_2, t_3)$ as defined in (80) we can deduce that $\mathrm{d}r_0 = \mathrm{d}t_1\, \mathrm{d}t_2\, \mathrm{d}t_3 |V|$. Therefore

$$\begin{aligned}
\lambda(n, m, l) &= \int_0^1 \int_0^1 \int_0^1 e^{-i\boldsymbol{p}_{nml}\cdot\boldsymbol{r}_0(t_1,t_2,t_3)} f(\boldsymbol{r}_0(t_1, t_2, t_3))\, \mathrm{d}t_1\, \mathrm{d}t_2\, \mathrm{d}t_3 && (90)\\
&= \int_0^1 \int_0^1 \int_0^1 e^{-i2\pi(nt_1+mt_2+lt_3)} \gamma(t_1, t_2, t_3)\, \mathrm{d}t_1\, \mathrm{d}t_2\, \mathrm{d}t_3 && (91)
\end{aligned}$$

Recall in (89) that λ can be expressed with the Fourier transform of f, which in turn was defined in (84). According to Fourier transform theory, it is a well known result that

$$\lambda(n, m, l) = a_{nml} - ib_{nml}, \tag{92}$$

According to (69), the terms a_{nml} and b_{nml} are acquired by calculating the mean value $\frac{\langle AC\rangle}{2\pi}$ and $-\frac{\langle BC\rangle}{2\pi}$ respectively. Since λ is the array we simulated, we can now construct the contact pair correlation function

$$\begin{aligned}
\gamma(t_1, t_2, t_3) = &\sum_{(n,m,l)\in\mathbb{Z}^3} \lambda_R(n, m, l) cos(2\pi(nt_1 + mt_2 + lt_3))\\
&-\lambda_C(n, m, l) sin(2\pi(nt_1 + mt_2 + lt_3)).
\end{aligned} \tag{93}$$

This is an infinite sum, which cannot be implemented with our simulations. In order to have an idea of what the contact pair correlation function looks like, we need a finite sum. When examining the values of λ_R and λ_C, they get their most significant values close to the origin $(0, 0, 0) \in \mathbb{Z}^3$. When examining values further away from

the origin, we can see that the values are so small, that 0 is within the error interval. We want to find a suitable cutoff value N such that we can calculate the sum only for when

$$|\boldsymbol{p}_{nml}| < N. \tag{94}$$

When examining values for γ at different points (t_1, t_2, t_3) we can determine a value N for which the values of γ converge. We define convergence as being less than 10% difference of values for γ between $[N-1, N]$. Based on this definition we can determine that the smallest suitable cutoff value would be $N = 6$. Note that this applies only for small N values starting from $N = 1$ onward. Therefore we can get a pretty accurate approximation of the contact pair correlation function with only

$$\begin{aligned}\gamma(t_1, t_2, t_3) \approx \sum_{|\boldsymbol{p}_{nml}|<6} & \lambda_R(n, m, l) cos(2\pi(nt_1 + mt_2 + lt_3)) \\ & -\lambda_C(n, m, l) sin(2\pi(nt_1 + mt_2 + lt_3)).\end{aligned} \tag{95}$$

We know that in our lattice we have one atom when $(t_1, t_2, t_3) = (0, 0, 0)$, and the closest atom from that point is in $(t_1, t_2, t_3) = (0.25, 0.25, 0.25)$. We want to visualize the contact pair correlation function γ between these 2 points. Therefore I'm going to plot the graph

$$\gamma_1(t) = \gamma(t, t, t), \quad \text{s.t. } t \in [0, 0.25]. \tag{96}$$

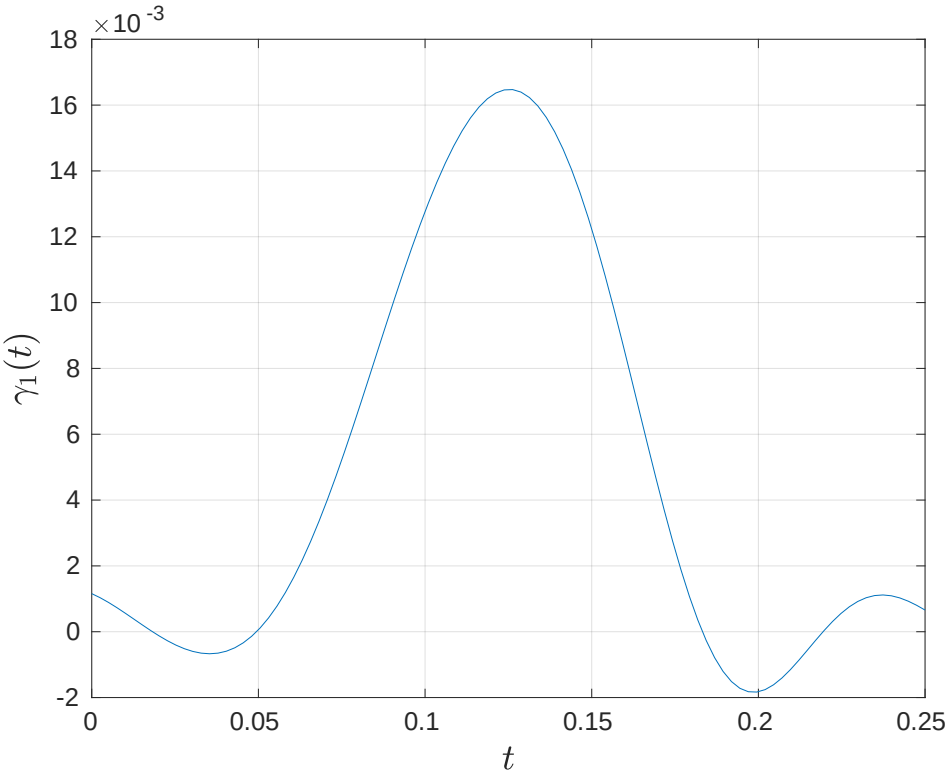

Figure 3: contact pair correlation function between two atoms

It is worth noting, that when N goes beyond 6, the graph of γ starts oscillating so much that it alters the general shape of the graph. The reasons for this will be explored in the conclusions. This graph can be compared with a prediction by the local-density approximation (LDA) as parametrized by Drummond, Ríos, Needs and Pickard in [3] by using equation (4):

$$\begin{aligned} g(0) =& 1 + 1.23r_s - 3.38208r_s^{3/2} + 8.6957r_s^2 - 7.37037r_s^{7/3} \\ &+ 1.75648r_s^{8/3} + 0.173694r_s^3 \end{aligned} \tag{97}$$

where

$$r_s = \sqrt[3]{\frac{3}{4\pi n_-}}, \tag{98}$$

where the electron density n_- as a function of position t that we acquired from the simulations. Details of this can be found in the CASINO manual [9] in chapter 34.2. With all this info, we can compare our results with the LDA results for the contact pair correlation function between two Si atoms. Since we are primarily interested with the shape of the curve instead of the absolute values, we have scaled the QMC result to coincide with the LDA one at the center of the Si-Si bond.

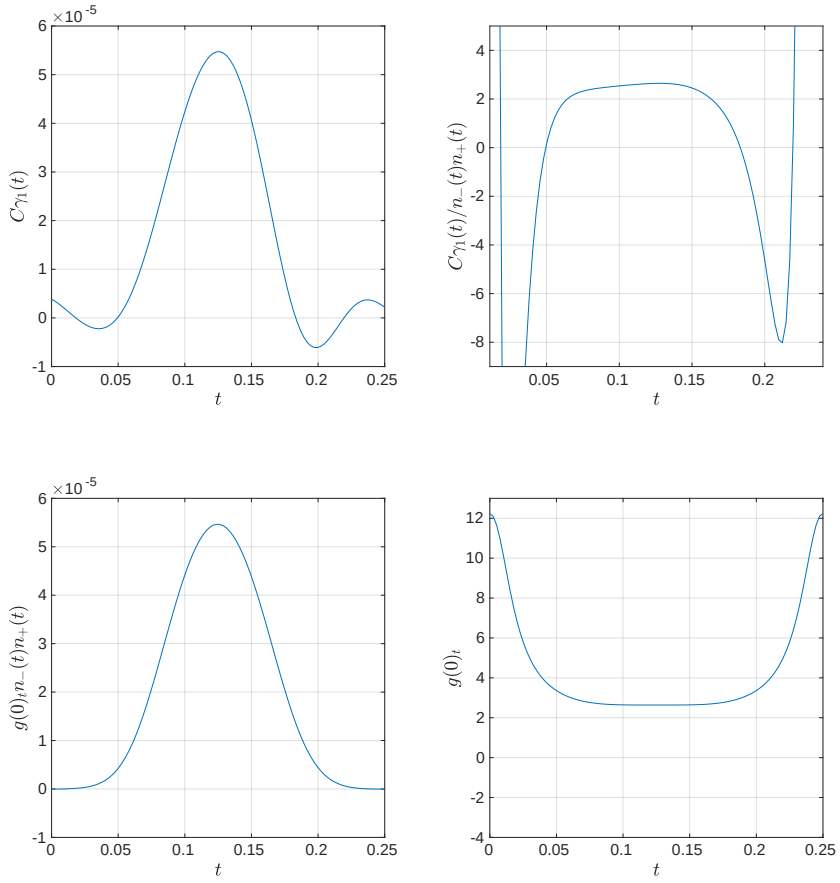

Figure 4: Our result for the re-scaled contact pair correlation function (upper left), the contact pair correlation function divided by the electron and positron densities, which is the enhancement factor (upper right), LDA enhancement factor's $g(0)_t$ product with electron and positron densities (lower left) and the LDA enhancement factor (lower right).

5 Conclusions

When comparing the LDA result and the results from this special assignment (figure 4) we can see that the graphs for $\gamma_1(t)$ and $g(0)_t n_-(t)n_+(t)$ are approximately similar. Recall that above we stated that when N goes beyond 6, the graph of γ starts oscillating so much that it alters the general shape of the graph. The reason for this can be because when making a sum of thousands of *sin* and *cos* functions with coefficients so small, that 0 is within the error interval, the total error of γ_1 adds up too much the bigger N gets. That's why we avoided using too many Fourier coefficients and keeping the cutoff radius N to a minimum. Another anomaly is that some values for γ_1 get negative values, which in theory is not desirable since the density of electrons at the positron is non-negative, which implies that the contact pair correlation function is non-negative as well. These negative values can be

explained with a combination of various factors. First, recall in (95) we didn't use an infinite sum as well as kept the cutoff radius N relatively small. Also even with a small cutoff radius, we have quite a few Fourier coefficients that are too close to 0, which can make the errors add up. These factors may explain why the contact pair correlation function γ_1 gets some negative values.

When comparing the enhancement factors $C\gamma_1(t)/n_-(t)n_+(t)$ and $g(0)_t$, we can see that both graphs rise as they go towards either edge, and reach a local minimum at the center. The difference is that in $g(0)_t$ the increase in values are a lot less steep. This difference can be explained by the fact that the values for the electron and positron densities $n_-(t)$ and $n_+(t)$ tend to zero toward the edges. Since we divide γ_1 with n_-n_+ it makes the values very high towards the edges. In addition the graph for $C\gamma_1(t)/n_-(t)n_+(t)$ makes a slight turn downward before rising when going towards the edge. This is simply because of the shape of $n_-(t)n_+(t)$. In addition, the LDA is just a simple model assuming that the enhancement factor at each point in space is the same as for a homogeneous electron-positron system with the densities equal to the local ones. This is not the case for our truly non-homogeneous system.

One more error could emerge when calculating the term S in (64). There is a good likelihood that many of the simulated values for r_{ij} get very close to 0, since in we use over 1 billion configurations, each of which simulate 64 positions for the electron. When using very small values for r_{ij}, their inverse value become extremely large. Then when summing them up and calculating their average, these extremely large values could distort the acquired average value quite a bit.

References

[1] E. Boroński and R. M. Nieminen. *Electron-positron density-functional theory*, volume 34. American Physical Society, Sep 1986.

[2] Dario Bressanini, Massimo Mella, and Gabriele Morosi. *Stability and positron annihilation of positronium hydride $L = 0, 1, 2$ states: A quantum Monte Carlo study*, volume 57. American Physical Society, Mar 1998.

[3] N. D. Drummond, P. López Ríos, R. J. Needs, and C. J. Pickard. *Quantum Monte Carlo Study of a Positron in an Electron Gas*, volume 107. American Physical Society, Nov 2011.

[4] N. D. Drummond, M. D. Towler, and R. J. Needs. *Jastrow correlation factor for atoms, molecules, and solids*, volume 70. American Physical Society, Dec 2004.

[5] W. M. C. Foulkes, L. Mitas, R. J. Needs, and G. Rajagopal. *Quantum Monte Carlo simulations of solids*, volume 73. American Physical Society, Jan 2001.

[6] S. D. Kenny, G. Rajagopal, and R. J. Needs. *Relativistic corrections to atomic energies from quantum Monte Carlo calculations*, volume 51. American Physical Society, Mar 1995.

[7] Yukiumi Kita, Ryo Maezono, Masanori Tachikawa, Mike Towler, and Richard J. Needs. *Ab initio quantum Monte Carlo study of the positronic hydrogen cyanide molecule*, volume 131. 2009.

[8] Richard M. Martin. *Electronic structure: Basic Theory and Practical Methods*. Cambridge University Press, Nov 2004.

[9] R. J. Needs, M. Towler, N. D. Drummond, and P. López Ríos. *CASINO User's Guide Version 2.13 (2015)*. 2019.

[10] Filip Tuomisto and Ilja Makkonen. *Defect identification in semiconductors with positron annihilation: Experiment and theory*, volume 85. American Physical Society, Nov 2013.